Cerebral Cortex December 2008;18:2719–2728
doi:10.1093/cercor/bhn050
Advance Access publication April 18, 2008

FEATURE ARTICLE
An Additional Motor-Related Field in the Lateral Frontal Cortex of Squirrel Monkeys

Numa Dancause[1], Vanja Duric[2], Scott Barbay[3,4,5], Shawn B. Frost[3,4,5], Antonis Stylianou[5] and Randolph J. Nudo[3,4,5]

[1]Department of Neurology, University of Rochester Medical Center, 601 Elmwood Ave, Box 673, Rochester, NY 14642, USA, [2]Department of Psychiatry, Yale University School of Medicine, 34 Park Street, Room S304, New Haven, CT 06519, USA, [3]Department of Molecular and Integrative Physiology, [4]Kansas Intellectual and Developmental Disabilities Research and [5]Landon Center on Aging, Kansas University Medical Center, 3901 Rainbow Blvd., Kansas City, KS 66160, USA

Our earlier efforts to document the cortical connections of the ventral premotor cortex (PMv) revealed dense connections with a field rostral and lateral to PMv, an area we called the frontal rostral field (FR). Here, we present data collected in FR using electrophysiological and anatomical methods. Results show that FR contains an isolated motor representation of the forelimb that can be differentiated from PMv based on current thresholds and latencies to evoke electromyographic activity using intracortical microstimulation techniques. In addition, FR has a different pattern of cortical connections compared with PMv. Together, these data support that FR is an additional, previously undescribed motor-related area in squirrel monkeys.

Keywords: frontal lateral cortex, frontal rostral area, intracortical microstimulation, motor control, neuroanatomy, ventral premotor cortex

Introduction

In the cerebral cortex, premotor areas are defined as frontal areas that have direct access to primary motor cortex (M1) and the spinal cord (Fulton 1935; Dum and Strick 2002). Accordingly, several premotor areas have been identified, primarily in macaque monkeys. Most medially, the cingulate motor areas (CMAs) are buried in the banks of the cingulate sulcus (Morecraft and Van Hoesen 1992; Picard and Strick 1996). Progressing laterally, the supplementary motor area (SMA), dorsal premotor (PMd), and ventral premotor (PMv) areas are found.

Each premotor area is interconnected with a panoply of different cortical fields, forming a network of structures that subserves planning and execution of movement. The distinctive anatomical connections of each premotor area suggest some specialization in their role as sensorimotor integration and motor output construction platforms. More particularly, PMv is part of a broad intracortical sensorimotor network integrating many sensory inputs (Tanné-Gariépy et al. 2002). Of all premotor areas, PMv is particular in its role in the visual integration of the target shape and configuration of the hand in accordance with this information (Murata et al. 1997). Phylogenetic, microstimulation, single unit recording and hodological studies suggest that PMv is at the center of an extensive network involved in processing of orofacial sensory inputs, motor control of the head and face and coordination of hand and orofacial movements (Wise 2006).

In prior studies, we documented the pattern of cortical connections of the PMv distal forelimb representation (DFL) in squirrel monkeys (Dancause, Barbay, Frost, Plautz, et al. 2006). These results revealed previously unidentified connections with a small field immediately rostral and ventral to the PMv DFL, an area we refer to as the frontal rostral area (FR). In the present publication, we provide electrophysiological and neuroanatomical evidence to suggest that FR is a separate motor-related area of the frontal cortex of this species. Based on its physiological properties and cortical connections, FR should not be considered a premotor area per se, but rather as an interface between the prefrontal, anterior opercular cortex and premotor areas, mainly PMv.

Materials and Methods

Surgical Procedures

Four adult, male squirrel monkeys (*Saimiri* spp.) were used, ranging in weight from 937 to 1255 g. All animal use was in accordance with a protocol approved by the Institutional Animal Care and Use Committee of the University of Kansas Medical Center. The surgical and neurophysiological procedures, as well as injections of neuronal tracers were effected on the hemisphere contralateral to the preferred hand on a reach-and-retrieval task (Nudo et al. 1992; Dancause, Barbay, Frost, Plautz, et al. 2006). Surgeries were performed using aseptic techniques and halothane-nitrous oxide anesthesia. Following a craniectomy and durectomy over the lateral portion of the frontal cortex, a plastic cylinder was fitted over the opening and used to contain warm, sterile silicone oil. In squirrel monkeys, we took advantage of the relatively lissencephalic cortex, which facilitates the construction of 2-dimensional physiological maps and coregistration of neuroanatomical data. A digital photograph of the exposed cortex was taken and subsequently used to create a 2-dimensional map of motor representations superimposed on the vascular landmarks. For the electrophysiological procedures, the halothane was withdrawn and ketamine–acepromazine or ketamine–valium (diazepam) was administered intravenously, as needed to maintain a stable anesthetic state. Anesthetic depth was inferred from general responsivity (e.g., pupils were constricted and the animal did not produce a blink reflex when the eyebrows or eyelashes were gently touched), muscle tone, heart and respiration rates. Neurophysiological procedures were conducted only during periods of stable anesthetic state. They were halted during occasional periods of shallow anesthesia, marked by responsiveness to cutaneous stimuli, excessive muscle tone in forelimb muscles combined with rapid heart and respiration rates or during occasional periods of deeper anesthesia, marked by the opposite physical signs and unusually high thresholds for evoking movements via intracortical microstimulation (ICMS) (Nudo et al. 1992, 2003). After the experimental procedures, animals were put back on halothane-nitrous oxide anesthesia for the injections of neuronal tracers (cases 472 and 1884) and aseptic closing of the craniectomy.

Derivation of Motor Maps

ICMS techniques were used to derive neurophysiological maps of movement representations of the DFL of M1, PMv, and FR. A microelectrode, made from a glass micropipette tapered to a fine tip and filled with 3.5 M NaCl (500- to 800-kΩ impedance), was used for electrical stimulation applied at a depth of ~1750 μm (layer 5). Stimulation consisted of a 40-ms train of 13 monophasic cathodal

pulses of 200 μs delivered at 350 Hz from an electrically isolated, constant current stimulator (Nudo et al. 1992; Dancause, Barbay, Frost, Plautz, et al. 2006). Pulse trains were repeated at 1-Hz intervals. In both M1 and PMv, current was ≤30 μA. If no movement was identified at 30 μA, the site was considered to be nonresponsive. In FR, somewhat larger stimulation intensities were often necessary to evoke movements, and thus, maximum current was increased to 80 μA. However, these stimulation currents are in line with what has been used in other studies of premotor areas in New World primates (Preuss et al. 1996). Because these different maximal stimulation intensities were used, it is possible that the M1 and PMv DFL areas may have been slightly underestimated. In particular, the caudal border of M1 DFL, along the area 4/3a border, is typically formed by nonresponsive sites. Nevertheless, the thresholds increase rapidly at the area 4/3a border. The 30 μA cutoff corresponds to the histologically defined area 4/3a border and thus the area 4 caudal border is probably fairly accurately described using the 30 μA stimulation limit (Nudo et al. 1992). Other borders of M1 and most borders of PMv were not comprised of nonresponsive sites. Only case 392 and 472 had limited PMv DFL bordered by nonresponsive sites (see Fig. 1). Thus, it is likely that the DFL area would not dramatically change using the 80 μA instead of the 30 μA intensity.

The cortical regions of interest were explored with microelectrode interpenetration distances of ~250–500 μm. For each motor area (i.e., M1, PMv, and FR), we included in the DFL all sites at which electrical stimulation elicited movements of the digits, wrist or forearm (pronation and supination). Sites at which the stimulation elicited movements of the elbow (flexion and extension), shoulder, orofacial or no response determined the physiological border of the DFL. Following these criteria, M1, PMv, and FR DFLs formed 3 well-isolated clusters. Movements were described using conventional terminology (Gould et al. 1986). Joint movements consequent to the electrical stimuli were indicated on the digital photograph at the precise locations of the electrode penetrations. The DFLs were defined by these evoked responses and their borders specified on the photograph. A custom-designed computer program was used to unambiguously circumscribe sites whose stimulation-evoked movements of the same category (e.g., digit, wrist/forearm) (Nudo et al. 1992). The cortical surface areas occupied by each movement category in the representational maps were then color-coded and analyzed using an image analysis program (Scion IMAGE, version 1.63. Frederick, MD). One animal (392) recovered from an experimental cortical infarct in M1 prior to the mapping of FR and thus, this animal was excluded from the quantitative analysis of representation areas, thresholds and EMG latencies. In 1 animal (1884), additional mapping was done to identify the location of DFLs of PMd and SMA to verify functional topography for neuroanatomical registration.

Electromyographic Data Collection and Analysis

In 2 animals (472 and 1884), following the ICMS mapping, bipolar surface electromyographic (EMG) sensors (Noraxon, Scottsdale, AZ) were positioned on the forelimb. Because the stimulation thresholds for movement onset in FR were higher than in other motor fields, we used this area to establish a case-specific reference stimulus intensity that consistently evoked EMG activity, and then used that same stimulus intensity in M1 and PMv. In case 472, we recorded evoked EMG activity resulting from stimulation of 2 sites in FR. We used the FR site that required the highest stimulation intensity to evoke a forelimb movement to define the reference stimulus intensity. The electrode was positioned in FR and the stimulation current was increased until an EMG signal could be evoked reliably (>50% of stimulation trains) and the signal-to-noise ratio was visually acceptable. The same current intensity obtained at this site in FR was then used at the other site in FR as well as at each of 2 PMv and M1 sites. For case 1884, the EMG data were collected in a similar manner from a total of 3 stimulation sites, 1 each in the middle of FR, PMv, and M1 DFLs.

Following $r_0=\sqrt{\frac{i}{k}}$, where r_0 is the radius of the cortical volume containing directly activated cells, i is the stimulus current, and k is the proportionality constant (Stoney et al. 1968), the use of similar current intensity in each area insured that we stimulated the same cortical volume at each site. Accordingly, the latencies we report are to a large

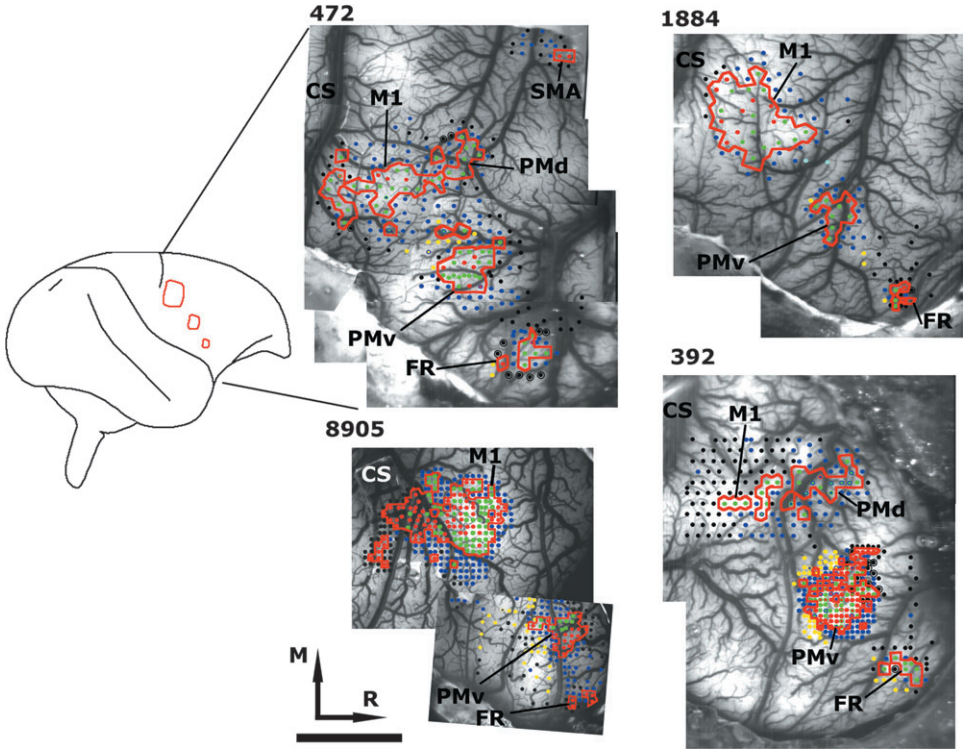

Figure 1. Reconstruction of ICMS movement maps. Digit and wrist/forearm movements comprised the DFL, indicated with a red contour. Each dot represents a microelectrode penetration site. The location of the ICMS-defined motor fields in each case is identified. Case 392 recovered from an experimental lesion in M1 prior to ICMS mapping explaining the small M1 DFL representation. Black dots = nonresponsive; black dots with large ring = site that was tested twice and still did not evoke response; dark blue = proximal movements; light blue = neck/back; green = wrist/forearm; red = digit; yellow = orofacial; R = rostral; M = medial; CS = central sulcus; scale bar = 5 mm.

extent representative of the density and size of layer 5 corticofugal neurons stimulated at sites within this fixed volume in each cortical area and the synaptic efficacy of the activated axons on their target neurons.

The EMG acquisition was synchronized with the stimulation train and sampled at 5 kHz through a 16-bit data acquisition card controlled with LabView custom software (National Instruments, Austin, TX). Data sets were analyzed using MATLAB (Mathworks, Natick, MA). The EMG records were rectified and low-pass filtered at a cut-off frequency of 50 Hz. A threshold method was then used to detect the onset of muscle activity, and thus the latency relative to the onset of the stimulation pulse train. For each individual trace, the mean plus 3 standard deviations of 1000 prestimulus EMG points was used as the threshold. To determine the onset of muscle activity, a 50-point sliding window (10 ms) was created and onset was defined as the 1st point of the window if all points in the window were above the threshold. By ensuring that at least 50 consecutive points are above the threshold, fluctuations of the EMG activity that could give a false onset are avoided.

EMG records where the algorithm was unable to detect a muscle onset were removed from further analysis. This condition occurs when the signal-to-noise ratio approaches unity and therefore accurate detection of the onset is not possible. The EMG records were also visually inspected and any cases where the muscle onset was detected before the stimulation or beyond 100 ms from the stimulus were rejected. This was done to ensure that muscle activity from involuntary contraction, which was not associated with the stimulus, was excluded from statistical analysis. After elimination of rejected EMG records, the average latency for each site was calculated.

Injections of Neuroanatomical Tracers

In 2 cases (472 and 1884), biotinylated dextran amine (BDA; 5% BDA in saline solution; 10 000 MW conjugated to lysine; Molecular Probes Eugene, OR) was injected into the center of the FR DFL to visualize anterograde and retrograde connectivity. All injections were made at multiple depths (100 nL at 1754 μm, 50 nL at 975 μm and 50 nL at 500 μm; Total injected volume 0.2 μL), in order to label a column of cortex through all 6 layers of the gray matter. Injections were made via pressure injection with a microsyringe pump controller (UPP2-1, WPI instruments), with a 1 μL Hamilton syringe through a tapered, graduated micropipette. Using similar methods, an additional injection of the fluorescent tracer Fast Blue (2% in H_2O; Dr. Illing Plastics GmbH, Gross-Umstadt, Germany) was made in the PMv DFL of case 472, to allow qualitative comparison of the pattern of connections of FR and PMv within the same animal (200 nL at 1754 μm, 100 nL at 975 μm and 100 nL at 500 μm; total injected volume = 0.4 μL).

Tissue Preparation

Twelve days following tracer injection, the animal was euthanized with a lethal dose of Euthasol (390 mg pentobarbital sodium/50 mg phenytoin sodium per 100 mL) injected intra-abdominally. The animal was perfused with 0.2% heparin/lidocaine in a 0.9% saline solution followed by 3% formaldehyde in phosphate buffer (pH 7.4), the brain removed and the cerebral cortex separated from the rest of the brain. The temporal and occipital lobes were then removed and the remaining parietal and frontal cortex flattened (Gould and Kaas 1981; Dancause, Barbay, Frost, Plautz, et al. 2006). The cortical block was sectioned tangential to the cortical surface (thickness 50 μm). Every 3rd section was used for histological processing to examine the presence of BDA. Other sections (1/3) were used for a myelin staining protocol (Gallyas 1979; Dancause, Barbay, Frost, Plautz, et al. 2006), to aid in the determination of boundaries mainly in the parietal cortex. The remaining sections were used for the analysis of the fluorescent neuronal tracing reagent Fast Blue. For a more detailed description of histological and anatomical methods see (Dancause, Barbay, Frost, Plautz, et al. 2006).

Quantitative Neuroanatomical Analyses

A neuroanatomical reconstruction system, consisting of a computer-interfaced microscope (Carl Zeiss, Thornwood, NY) and associated software (Neurolucida, Microbrightfield, Williston, VT), was used to record the locations of labeled terminals and cell bodies.

Documentation of Terminal Labeling

A varicosity was considered to be a terminal bouton if it appeared as a small, darkly labeled sphere contacting a small fiber. For all cases, high-resolution photographs of the BDA-processed sections were acquired using a MicroLumina digital scanning camera (Leaf Systems, Westborough, MA) and imported into Photoshop (Adobe Systems, San Jose, CA). These photographs were scanned visually (but not entered into the computerized neuroanatomical system). As in other publications (Dancause et al. 2005, 2007; Dancause, Barbay, Frost, Plautz, et al. 2006; Dancause, Barbay, Frost, Plautz, Popescu, et al. 2006), qualitatively, terminal distribution was found to be consistent through depths approximately corresponding to layers 2–6 of the gray matter. Thus, for quantitative comparisons, 1 representative slide per animal was sampled at depths roughly corresponding to layer 5 (situated at depth ~1600–1800 μm). In this regard, it is necessary to keep in mind that tangential sectioning is particularly useful for the coregistration of physiological and anatomical data and provides very limited information concerning the cortical layers (see Dancause et al. 2007 for a discussion on this topic). Thus, our inability to find differences in distribution across sections reflects the limitations of the anatomical techniques and does not necessarily imply an absence of quantitative differences of terminal distribution across layers.

We sampled the selected slides using a grid pattern overlaid on the section image. If at least 2 terminals were located within a 100 × 100 μm square of the grid, at any depth within the section, a marker was placed in the center of the square. As each section had a finite depth (50 μm), the volumetric unit "voxel" is used in the present description. Accordingly, our quantitative report of the magnitude of FR projections to different areas does not reflect the density of the projections per se. The resulting numbers of labeled voxels are more correlated with the cortical volume occupied by terminals from FR. It is noteworthy that in other studies we found that the percentage of terminals was not significantly different from the percentage of cell bodies in any of the cortical regions and converting labeled voxel counts to voxels per mm^2 to control for the total surface area of a region of interest did not affect our results (Dancause, Barbay, Frost, Plautz, et al. 2006; Dancause et al. 2007). Together, these data suggest that the voxel method is a valid measure of the strength of projections.

Documentation of Neuronal Cell Body Labeling

Six sections ranging from 500- to 1850-μm depths per hemisphere were used to document the location of BDA labeled cell bodies and 4 sections were used to document Fast Blue labeled cell bodies in case 472. For cells to be considered as positively labeled with BDA, cell bodies needed to display a full rounded body in which black granules could be observed and the round body needed to show at least 2 protuberances, considered to be dendrites or the axon, also darkly stained (Dancause et al. 2005; Dancause, Barbay, Frost, Plautz, et al. 2006). For Fast Blue, the cells simply were required to contain the fluorescent tracer in their somata (Dancause et al. 2007). It should be kept in mind that BDA (10 000 MW) is not known to be a particularly effective retrograde neuronal tracer (Reiner et al. 2000). However, in previous studies we found that labeled cell bodies and terminals were colocalized in all areas of the cortex (Dancause et al. 2005, 2007; Dancause, Barbay, Frost, Plautz, et al. 2006). Thus, whereas the cell body counts obtained with this tracer cannot be considered as a complete representation of the numbers of cells projecting to the zone of injection, the percentage of cells found in each cortical area should still provide information concerning the proportion of inputs to FR from the diverse cortical areas. We chose to maximize visualization of projections (terminal boutons) of FR using BDA (10 000 MW) in the present study to allow appropriate comparison with our group of animals in which the same tracer was injected in PMv (Dancause, Barbay, Frost, Plautz, et al. 2006). In addition, BDA (10 000 MW) is known to produce confined injection cores (Dancause, Barbay, Frost, Plautz, et al. 2006), a factor that is particularly crucial when considering the size of the FR DFL representation we targeted (see below).

Blood vessel patterns were utilized to align section reconstructions with photographs of myelin stained sections and with physiological

map data (Dancause et al. 2005). Tangential sectioning aided this alignment procedure and allowed precise identification of the location of neuronal labeling (Dancause, Barbay, Frost, Plautz, et al. 2006). Neuroexplorer (Microbrightfield, Williston, VT) was used to report exact counts of cell bodies or voxels in different areas of the brain. To account for differences due to injection size, numbers of terminal voxels and cell bodies were transformed to percentages (Dancause et al. 2005; Dancause, Barbay, Frost, Plautz, et al. 2006).

The distribution of connections was documented by dividing the hemisphere into the same 14 cortical regions used in earlier reports in the same species (Dancause, Barbay, Frost, Plautz, et al. 2006; Dancause et al. 2007). Area locations were based on physiological documentation, myelin staining, anatomical landmarks and comparison with other physiological and anatomical studies (Preuss and Goldman-Rakic 1989; Krubitzer and Kaas 1990; Jain et al. 2001). Labeling located between PMv and SMA clusters was attributed to PMd. All labeling medial to SMA was considered to be within CMAs. The operculum was divided into posterior operculum/inferior parietal cortex (PO/IP) and anterior operculum (AO): PO/IP was the operculum caudal to the hand/face septum and AO was the operculum rostral to the hand/face septum. Any labeling caudal to S1 and medial to PO/IP was included in PP. The identification of functional areas that were located outside of the neurophysiologically and neurohistochemically defined borders was limited and was primarily based upon topographic location and similarities to results of previous tract-tracing studies. Whereas this limitation should be kept in mind, the consistency in the overall pattern of label across cases allows us to be relatively confident of our approximations.

For comparison, we restricted the analysis to the pattern of ipsilateral connections outside PMv or FR, depending upon the location of the injection. Thus, in all cases, the percentage of connections to different areas was calculated as follows:

$$\frac{\text{Total } L \text{ in area } X}{\text{Total } L \text{ in hemisphere} - \text{Total } L \text{ in area } k}$$

where L = number of terminal voxels or cell bodies, and X = cortical area of interest, k = site of injection that is, FR or PMv.

The quantitative analysis of the pattern of connections of PMv and FR was based on the data of 4 cases with BDA (10 000 MW) injections in PMv DFL (data from Dancause, Barbay, Frost, Plautz, et al. 2006) and the 2 cases in the present study with injection of the same tracer in FR DFL. The Fast Blue injection in PMv was used only for qualitative representation of the pattern of connections of PMv and FR within a single animal. These data were not used for quantitative comparison of the pattern of connections because they were made with different tracers (FB and BDA [10 000 MW]), labeling different anatomical structures (cell bodies and terminals) and a different volume of tracer was injected (0.4 μL for FB versus 0.2 μL for all BDA injections), rendering the quantitative comparison of the pattern of connections resulting from these injections difficult.

Results

Localization of M1, PMv, and FR DFL

Figure 1 illustrates the ICMS results used to define the DFL of various motor fields of the frontal cortex from 4 animals. As in previous studies in squirrel monkeys, M1 DFL was found immediately rostral to the central sulcus (Strick and Preston 1982; Donoghue et al. 1992; Nudo et al. 1992). The caudal border of M1 DFL was defined by unresponsive sites near the border between area 4 and area 3a. The medial, lateral and rostral borders of M1 DFL were defined by evoked movements of proximal joints.

The PMv DFL was located rostral and lateral (ventral) to M1 DFL (Frost et al. 2003; Dancause, Barbay, Frost, Zoubina, et al. 2006). The M1 and PMv DFLs were typically separated by proximal (i.e., shoulder and elbow) and orofacial representations (average distance between M1 and PMv DFL borders ± SD = 3.29 ± 0.46 mm). The PMv DFL was bordered by orofacial representations caudally and laterally and proximal representations rostrally and medially (Frost et al. 2003; Dancause, Barbay, Frost, Zoubina, et al. 2006). Both M1 and PMv DFLs each contained a single, contiguous representation, but sometimes were divided into smaller islands by proximal representations. However, the distance between these islands did not exceed 500 μm.

A 3rd, spatially distinct DFL, here called FR, consistently was found further rostal and lateral to PMv (distance between FR and PMv DFL borders ± SD = 2.45 ± 0.82 mm and between FR and M1 DFL borders = 8.00 ± 0.74 mm). At the caudal border of FR DFL, orofacial movements were often evoked. Otherwise, borders consisted of nonresponsive and proximal sites. The size of the M1 DFL was 10.8 mm^2; PMv DFL was 3.1 mm^2 or less than 1/3 the size of M1 DFL; FR DFL was 0.9 mm^2, or less than 1/3 the size of PMv DFL (Fig. 2*A*).

Thresholds for Evoking Movements in M1, PMv, and FR

The average current to elicit movements of the upper extremity using ICMS was higher in FR (mean ± SEM = 51.3 ± 1.87 μA) compared with PMv (16.5 ± 1.11 μA) and M1 (12.2 ± 7.9 μA; Fig. 2*B*). ANOVA revealed that the main effects of Area (i.e., M1, PMv, and FR) and Movement Type (i.e., digits, wrist/forearm, and proximal) on threshold were statistically significant (F = 191.90, P < 0.0001 and F = 8.57, P = 0.0002, respectively). The interaction term was also significant (F = 3.73, P = 0.0053). Post hoc analysis (Fisher's least significant difference test with alpha set at 0.05) revealed that FR thresholds were significantly higher than either PMv or M1 thresholds and PMv thresholds were significantly higher than M1 thresholds. Within FR, the thresholds for wrist/forearm (least square mean ± SEM = 62.6 ± 3.7 μA) movements were significantly higher than proximal (51.3 ± 2.1 μA) and digit movements (39.9 ± 3.7 μA) and thresholds for proximal movements were significantly higher than digit movements.

EMG Latencies in M1, PMv, and FR

In 2 cases we collected ICMS-evoked EMG activity in the contralateral forelimb (Fig. 2*C*). Because current thresholds for eliciting movement were higher in FR compared with PMv and M1, FR was used to establish a standard current level for evoking reliable EMG in each case, as described in Methods. First, in case 472, EMG activity was recorded from the forearm extensor compartment as a result of 30 μA ICMS. A total of 263 stimulation-evoked EMG trials were obtained from 2 sites in M1, 237 trials from 2 sites in PMv and 109 trials from 2 sites in FR. As shown in Table 1, the average latency for FR sites was higher than PMv or M1.

Next, in case 1884, EMG activity was recorded from the arm flexor compartment (biceps) as a result of 80 μA ICMS. A total of 120 stimulation-evoked EMG trials were obtained from 1 site in M1, 120 trials from 1 site in PMv and 125 trials from 1 site in FR. As in case 472, the latency to onset of EMG activity was higher in FR compared with PMv or M1 (Table 1). The shorter latencies found in this case in comparison to case 472 can probably be attributed to the higher stimulus intensity that was required and/or the muscle compartment from which the EMG was recorded.

To pool data of the 2 animals together, we normalized the FR and PMv latencies relative to average latencies in M1 for each

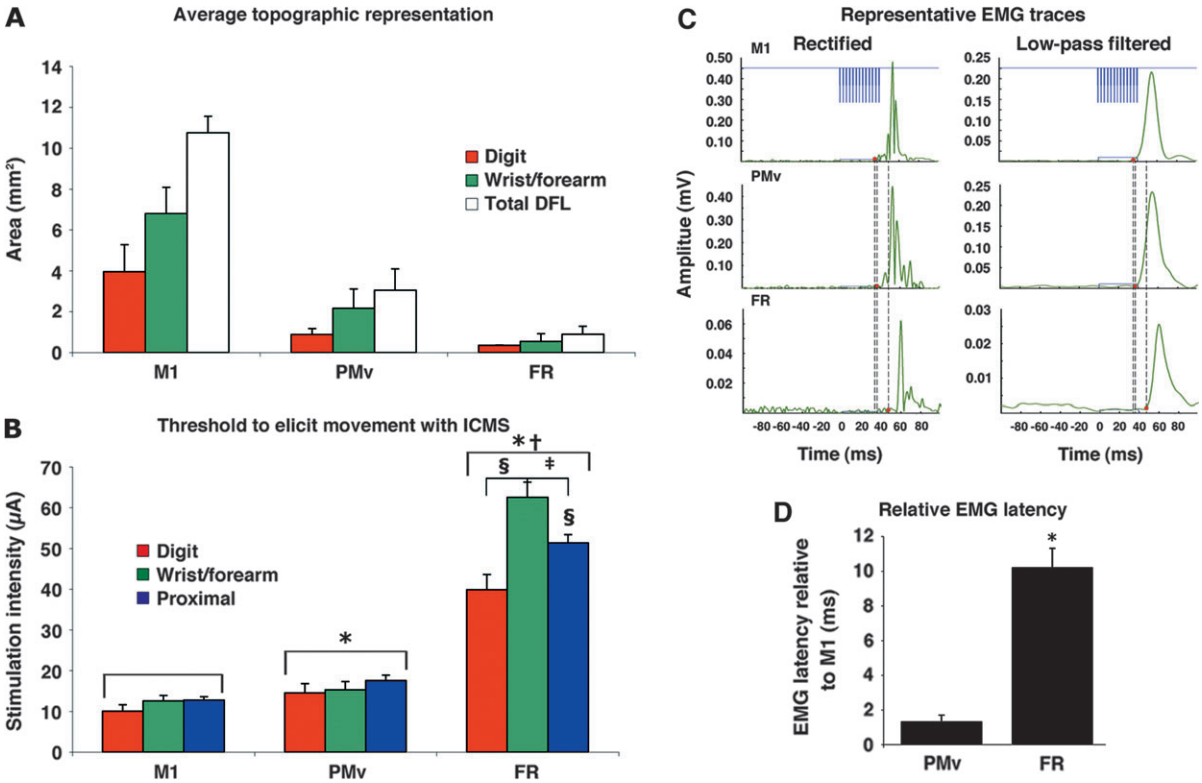

Figure 2. Area, threshold and latency for ICMS-defined representations in M1, PMv, and FR. (*A*) ICMS-evoked movement representations within the DFL of 3 motor fields: M1, PMv and FR (mean area ± SEM). The cortical surface area devoted to component movements is depicted. M1 DFL was more than 3 times larger than PMv, whereas PMv DFL was more than 3 times larger than FR. However, the proportion of component movements within each of these fields was similar. Monkey 392 was excluded from quantitative analysis because this subject had been given an M1 lesion. (*B*) Thresholds at which movements could be evoked using ICMS in M1, PMv, and FR (mean intensity ± SEM). Again this analysis excluded monkey 392. Statistical analysis revealed that movement thresholds in M1 were significantly lower than PMv and FR (*) and that thresholds in PMv were lower than FR (†). Within FR, digit movement thresholds were significantly lower than proximal and wrist/forearm (§). In addition, wrist/forearm movement thresholds were significantly higher than proximal movements thresholds (‡). (*C*) Representative ICMS-evoked EMG traces from each cortical area (M1, PMv and FR) recorded from the forearm extensors in case 472. On the left, the rectified traces are unfiltered. On the right, the same traces are shown following low-pass filtering, which were subsequently used for defining EMG onset. The train of stimulation is shown in blue (top). For each inset, the EMG trace is in green and the duration of the stimulation is in blue. A double dotted line identifies the onset of evoked EMG activity from M1 and PMv stimulation and the single dotted line identifies the onset of evoked EMG activity from FR stimulation. The *y*-axis is auto-scaled for the maximum amplitude of each trace. (*D*) Average latencies to evoke EMG activity with ICMS in PMv and FR relative to latencies in M1 (mean latency ± SEM). Within each monkey, the PMv and FR latencies were normalized by arithmetic subtraction from M1 latencies so that the data from both animals could then be combined (case 472, 2 PMv sites and 2 FR sites; case 1884 1 PMv site and 1 FR site). Normalized latencies to evoke EMG from FR were significantly longer than from PMv (*indicates statistically significant difference at $P < 0.05$).

Table 1
Latency of ICMS-evoked EMG activity

Animal	Stimulation site	Cortical region	Muscle group	Intensity (μA)	Average latency (ms)[a]	SEM (ms)	Latency difference from M1 (ms)
472	31	FR	Dorsal forearm	30	48.18	1.14	12.40
472	35	FR	Dorsal forearm	30	45.12	0.45	9.34
472	105	PMv	Dorsal forearm	30	36.43	0.48	0.66
472	113	PMv	Dorsal forearm	30	37.00	0.46	1.22
472	172	M1	Dorsal forearm	30	34.95	0.41	N/A
472	177	M1	Dorsal forearm	30	36.6	0.34	N/A
1884	52	FR	Biceps	80	23.83	0.63	8.83
1884	28	PMv	Biceps	80	17.03	0.42	2.03
1884	58	M1	Biceps	80	15.00	0.29	N/A

[a]It is likely that both the different stimulation intensities used as well as the different muscles group recorded contributed to the large differences in latencies found in the 2 animals.

animal (arithmetic difference; Fig. 2*D*). Although PMv latencies were nearly equivalent to M1 latencies, FR latencies were about 10 ms longer than M1 latencies. A 2-tailed *t*-test between PMv (3 stimulation sites) and FR relative latencies confirmed that latencies to evoke EMG activity with FR stimulation were significantly longer ($t = 7.513$; $P = 0.0215$).

Because we used identical current intensity across stimulation sites within each case, the intensities relative to threshold current levels were much larger in M1 compared with those used in FR. However, the M1 latencies we found do not appear to be substantially different from other EMG studies in squirrel monkey (Strick and Preston 1982; Donoghue et al. 1992). Thus,

the significant difference in EMG latencies among areas is probably not a function of substantially larger numbers of corticospinal neurons (CSNs) that were activated in different areas. In addition, whereas our latency results are extrapolated from a limited number of cortical stimulation sites, the large latency differences between PMv and FR and the small standard error suggest that the differences in latencies found between the areas are representative. Nonetheless, due to the limitations of the methods used, results concerning latency should not be considered as a definitive statement about this property of FR.

Ipsilateral Cortical Connections of FR

In 2 animals (472 and 1884), injections of BDA (10 000 MW in saline) were made in the centers of the FR DFL to trace its cortical connections. Reconstruction of the BDA injection cores confirmed that they were located within the majority of the DFL of FR in both cases and that the cores were of typical size for the injected volume using similar methods (472 = 1.41 mm^2; 1884 = 0.73 mm^2) (Dancause, Barbay, Frost, Plautz, et al. 2006). However, due to the irregular shape and the small size of FR, the core encroached slightly on proximal representations in case 472, and both proximal representations and non-responsive area in case 1884.

As in previous studies (Dancause, Barbay, Frost, Plautz, et al. 2006; Dancause et al. 2007), labeled cell bodies and terminals were colocalized, supporting the reciprocity of connections. Only terminal distribution patterns are illustrated here for simplicity (Fig. 3; see cell body data in Table 2). In the prefrontal cortex, labeling was found rostral to FR, in areas designated as "frontal other" (FO), in the region corresponding to area 46. Additional extensive labeling was also found in AO, in the region corresponding to PrCO. Moderate labeling was present in PMv and CMAs. In both cases, sparse labeling was found in SMA, PMd and M1. In the parietal cortex, extensive labeling was found in PO/IP, specifically in regions corresponding to area 7b, the secondary somatosensory cortex (S2) and parietal ventral cortex (PV). Sparse labeling was found in the posterior parietal cortex (PP).

Comparison of FR and PMv Cortical Connections

The pattern of connections of FR derived from these 2 cases was compared with the pattern of connections of PMv derived from a previous study (n = 4; Dancause, Barbay, Frost, Plautz, et al. 2006). Figure 4*A* shows the distribution of projections following an injection of comparable size and depth, of BDA (10 000 MW) in the DFL of PMv (case 1934 from Dancause, Barbay, Frost, Plautz, et al. 2006). Following PMv injection, M1 was the most intensely labeled cortical area and relatively sparse labeling was found in FO. To provide within-case qualitative assessment of FR and PMv connections, an additional injection of Fast Blue was made in PMv DFL in case 472 (Fig. 4*B*). This comparison was made using different tracers (anterograde and retrograde) and thus, was not used for quantitative analysis. However, because the connections of both PMv and FR were reciprocal with all areas of the cortex (see Table 2), this figure provides useful qualitative information on how the patterns of connection of PMv and FR DFLs diverge within a single case. In particular, note the difference of connections with AO. This figure shows that, in comparison to PMv, FR has more connections with AO and its connections are found more rostrally in AO.

Finally, we quantitatively compared the pattern of connections of our 2 cases with FR DFL injections of BDA (10 000 MW), to the 4 cases in which the same tracer was injected in

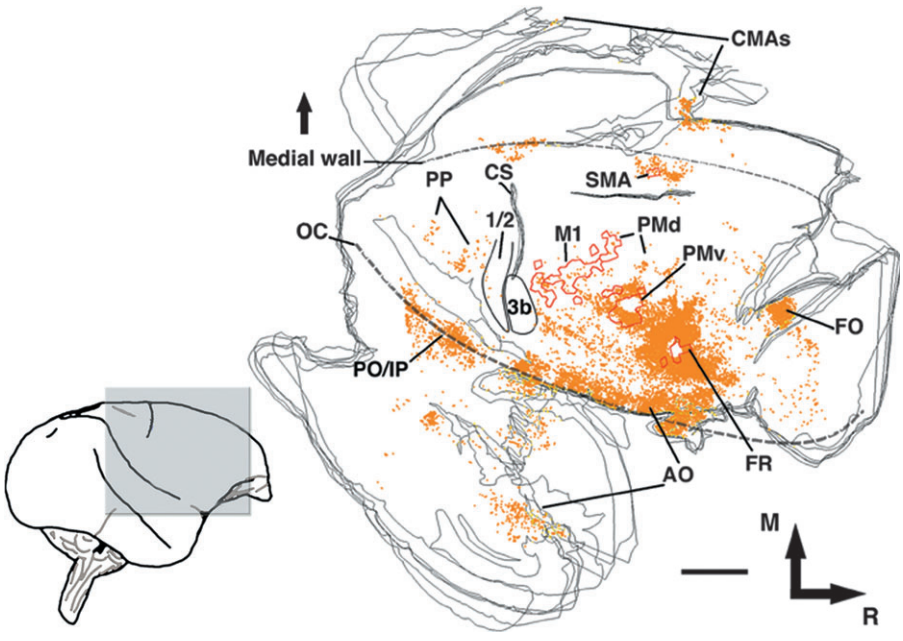

Figure 3. Pattern of connections of FR DFL in the ipsilateral hemisphere. Distribution of voxels with labeled terminals after injection of BDA into FR DFL (case 472; large injection; approximate depth of section = 1750 μm). This animal had the largest BDA injection in our 2 FR injected animals, which was of comparable size to the PMv injection in case 1934 (see Fig. 4*A*). Each orange dot represents a voxel (100 × 100 μm resolution; approximate depth 1500 μm) in which at least 2 labeled varicocities (terminal boutons) were identified. ICMS-defined DFLs are outlined with red contours and histochemically defined sensory areas (3b and area 1/2) in black contours. Additional dotted lines indicate the junction between the lateral and medial wall and the convexity of the lateral sulcus (operculum; OC). 1/2: primary somatosensory areas 1 and 2; 3b: primary somatosensory area 3b; CS: central sulcus; FO: frontal (others); M1: primary motor cortex; M = medial; R = rostral. Scale bar = 5 mm.

Table 2
Distribution of labeled cell bodies and voxels with labeled terminals

	FR injections								PMv injections			
	472 (0.2 μL of BDA)				1884 (0.2 μL of BDA)				472 (0.4 μL of FB)		Average (0.2 μL of BDA) from Dancause, Barbay, Frost, Zoubina, et al. (2006)	
	Cell body		Terminal		Cell body		Terminal		Cell body		Cell body	Terminal
Area	Raw	%[a]	Raw	%[a]	Raw	%[a]	Raw	%[a]	Raw	%[b]	% ± SD	% ± SD
PMv	129	9.1	677	9.5	163	18.6	306	7.2	†			
M1	12	0.8	105	1.5	0	0.0	34	0.8	2892	18.2	25.8 + 10.6	29.5 ± 4.17
PMD	3	0.2	97	1.4	2	0.2	59	1.6	747	4.7	6.0 + 4.2	5.8 + 2.1
SMA	28	2.0	170	2.4	7	0.8	103	2.8	2300	14.5	8.5 + 11.4	7.5 + 1.3
CMAs	9	0.6	334	4.7	7	0.8	259	7.1	650	4.1	0.7 + 0.6	2.6 + 0.8
FO	371	26.3	1185	16.6	177	20.3	1301	35.7	813	5.1	0.1 + 0.1	1.6 + 2.2
AO	420	29.7	2676	37.4	254	29.1	1065	29.2	2083	13.1	2.5 + 2.2	7.1 + 7.9
PO/IP	234	16.6	930	13.0	169	19.3	655	18.0	2612	16.5	15.3 ± 6.1	7.6 ± 4.4
PP	0	0.0	100	1.4	0	0.0	19	0.5	741	4.7	1.4 ± 1.5	1.4 ± 1.6
S1	1	0.1	67	0.9	2	0.2	40	1.1	257	1.6	2.1 ± 0.9	4.1 ± 2.7
FR	954		1102		1027		1651		2453	15.5	22.7 + 8.4	22.3 + 4.4
Total identified	2161	91.3	7443	90.2	1808	95.1	5492	93.0	15 554	98.0		
Nonidentified	205		809		93		411		314			
Gross total	2366		8252		1901		5903		15 868			

Note. †PMv had an extremely high number of labeled cell bodies with Fast Blue in the injection halo and throughout the area. PMv cell bodies were only plotted in 1 section for graphic representation in Figure 5. Thus, total numbers for the PMv area are not available.
[a]Extrinsic percentages were obtained by dividing the number of cells or voxels in an area by the gross total − PMv or − FR (see text). It is also worth noting that the PMv labeling in case 472 was affected by the presence of the FB injection core. Thus, percentage of connections with PMv are most likely to be slightly underestimated in the present study.
[b]For the FB injection, the extrinsic percentages are obtained by dividing the number of cell in an area by the gross total because PMv value is equal to zero.

PMv DFL (data from Dancause, Barbay, Frost, Plautz, et al. 2006). In contrast to PMv, FR had substantially more connections with FO and AO and substantially fewer connections with M1. Whereas connections were present in all premotor areas, in contrast to PMv, FR had fewer connections with PMd and SMA and more connections with CMAs (Fig. 5 and Table 2).

Discussion

We have provided evidence that an additional, isolated, motor-related cortical representation, which we designated as FR, is located rostral and lateral to PMv in a New World primate, the squirrel monkey. Using ICMS, we found that the FR DFL is relatively small in comparison to PMv and M1 DFLs. Movements and EMG activity evoked from FR stimulation have higher thresholds and longer latencies (respectively) than those of PMv and M1. Tract-tracing results demonstrated that FR has dense connections with prefrontal cortex, anterior opercular areas and posterior operculum/inferior parietal cortex, moderate connections with PMv and CMAs, but relatively few connections with SMA, PMd, and M1. This is in contrast to PMv, which has dense connections with M1, but sparse connections with prefrontal areas (Dancause, Barbay, Frost, Plautz, et al. 2006). These data suggest that FR is a separate motor-related cortical field and might act as an interface between premotor areas, mainly PMv, and prefrontal/anterior opercular cortex.

Similarities between FR and PMv

Our data show that FR has a very similar topographic organization to other distal forelimb motor fields, especially PMv. We found a core of DFL surrounded by proximal forelimb representations. At threshold ICMS current levels, specific digit, wrist and forearm movements were evoked from FR, similar to those that were evoked from stimulation in other motor fields. Further, although significant differences in current thresholds were found between FR and PMv (and between FR and M1), these stimulation intensities were still relatively low (~40 μA for evoking digit movements). This indicates that the evoked distal forelimb movements were not the result of direct current spread into the nearby PMv DFL (Stoney et al. 1968).

Based on our anatomical data, it would appear that PMv and FR are largely part of the same cortical network. Both areas share connections with all other premotor areas. In addition, the majority of parietal connections for both PMv and FR are shared with PO/IP, that is, areas 7b, S2, and PV. The similarities in their patterns of connection and the dense connections between FR and PMv suggest that they might have shared functions in motor control, perhaps in the integration of sensory information and the translation of this information into appropriate motor output (Rizzolatti et al. 2001).

Differences between FR and PMv

The higher stimulation intensity to evoke movement and longer evoked EMG latencies from FR suggest that its role in motor output production is not as direct as for other motor areas. The output of FR most likely is carried through additional synapses, explaining the higher intensities and longer latencies.

The indirect influence of FR on motor output can also be suggested from its pattern of connections. A striking difference between the cortical networks of FR and other motor areas is its very sparse connections with M1. It is likely that FR has a weaker modulatory effect on M1, in comparison to PMv (Shimazu et al. 2004). Although anatomical studies of descending pathways have not focused on FR specifically, prior studies in squirrel monkeys revealed no CSNs in this area, despite large numbers of CSNs in areas corresponding to M1 and PMv DFL (region C of Nudo and Masterton 1990).

FR also has particularly prominent connections with the prefrontal cortex and AO. Together, these connections comprise a unique network among motor areas, that is thought to be involved in working memory (Petrides 1995; Owen 1997); in taste perception (Rolls 1989) and voluntary control of

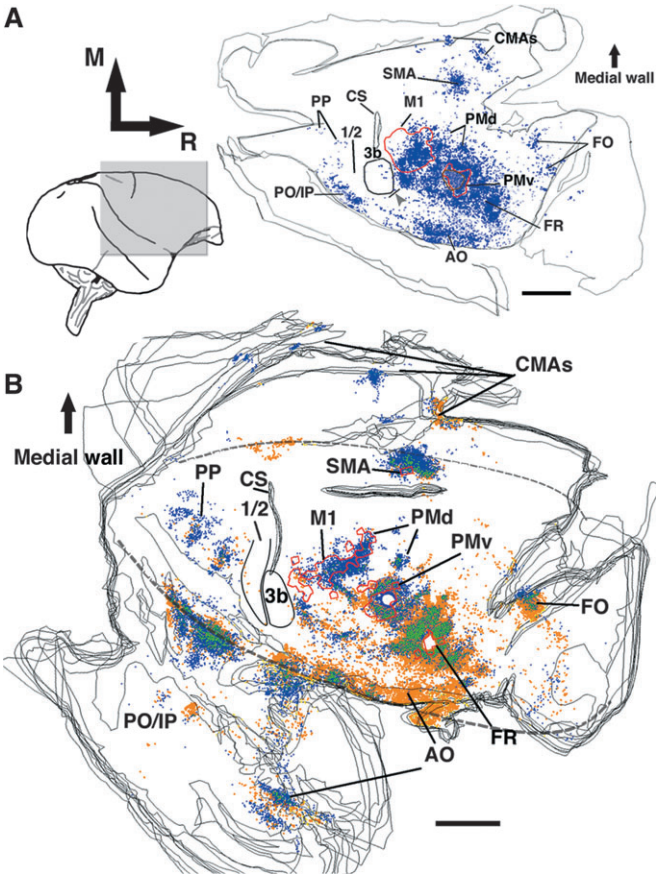

Figure 4. Comparison of the pattern of connections of PMv and FR DFL in the ipsilateral hemisphere. (*A*) Pattern of connections of PMv DFL in the ipsilateral hemisphere. Reconstruction of the typical distribution of voxels with labeled terminals observed in flattened, tangential sections through the fronto-parietal cortex in a case with a BDA injection in the PMv DFL (case 1934; Dancause, Barbay, Frost, Plautz, Stowe, et al. 2006). This injection was of comparable size and depth as the FR injection in case 472 (Fig. 3). As this animal received the largest BDA injection of any in that study, and displayed the most extensive and densest distribution of terminals, it provides a reasonable estimate of the limits of normal PMv connectivity. Each blue dot represents a voxel (100 × 100 μm resolution; approximate depth 1500 μm) in which at least 2 labeled varicocities (terminal boutons) were identified. ICMS-defined DFLs are outlined with red contours and histochemically defined sensory areas (3b and area 1/2) in black contours. In particular, note the intense BDA labeling found in M1 and the sparse labeling found in FO. In addition, BDA labeling in AO is less intense and more caudal than what was found following BDA injection in FR. (*B*) Within-case comparison of the pattern of connections of PMv and FR DFL in the ipsilateral hemisphere. Distribution of labeled terminals following injection of BDA into FR DFL (orange dots; see Fig. 3) and labeled cell bodies after injection of FB into PMv DFL (blue dots). One orange dot represents a voxel with labeled terminals and 1 blue dot represents a cell body. When both Fast Blue and BDA were colocalized, green is used. Abbreviations as in Figure 3. Scale bar = 5 mm.

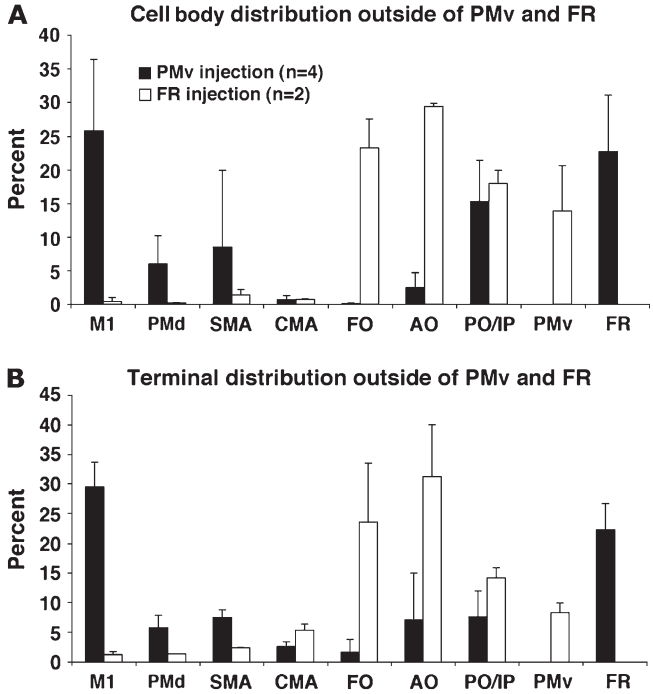

Figure 5. Quantitative distribution of labeling in the ipsilateral hemisphere. (*A*) Cell body distribution and (*B*) voxels with labeled terminals distribution following BDA injection in FR ($n = 2$) is compared with the distribution following injection in PMv ($n = 4$; from Dancause, Barbay, Frost, Plautz, Stowe, et al. 2006). Extrinsic connections with PMv are only available for the group of animals that had injection in FR and vice versa. Consequently, in these cases, to obtain the percentages, the denominator was the gross total — FR *or* PMv. It should be noted that the FR group is composed of only 2 animals and that the error bars simply show the variance between these 2 cases. See Figure 3 for abbreviations.

facial, oral and lingual movements (Mao et al. 1989). FR connections with these areas would be consistent with the particular role attributed to the PMv network in unimanual feeding behaviors (Wise 2006).

Evidence for FR in other Primate Species

In macaque monkeys, each premotor area has clear subdivisions (Vogt and Vogt 1919; Von Bonin and Bailey 1947; Matelli et al. 1985; Barbas and Pandya 1987). For example, PMd and SMA contain a rostral portion called pre-PMd (F7) and pre-SMA (F6) and a caudal portion called PMd proper (F2) and SMA proper (F3; Picard and Strick 2001). In general, the caudal subdivisions of PMd and SMA share more numerous connections with the primary motor cortex (M1) and have more corticospinal projections than their rostral counterparts (Dum and Strick 1991; He et al. 1993). In contrast, the rostral subdivisions have a more elaborated network with other frontal and prefrontal areas (Bates and Goldman-Rakic 1993; Luppino et al. 1993; Lu et al. 1994) and the current intensity necessary to evoke movements using ICMS is generally higher (Luppino et al. 1991; Matelli et al. 1991). Comparable subdivisions of PMd and SMA have also been reported in New World primates (cebus monkeys; Dum and Strick 2005) and owl monkeys (Preuss et al. 1996; Sakai et al. 2000) as well as in prosimian primates (galagos; Fang et al. 2005).

For PMv, cytoarchitectonic subdivisions into caudal (F4) and rostral (F5) parts have only been identified in macaques so far (Matelli et al. 1985). Furthermore, the hand representation of the macaque PMv is mainly found in the rostral part of PMv (F5) (Gentilucci et al. 1988; Rizzolatti et al. 1988) and is known to share dense and powerful connections with M1 (Matelli et al. 1986; Shimazu et al. 2004). In fact, the PMv DFL of squirrel monkeys and macaques (PMvr or F5) share many features such as comparable topographic organization (Kurata and Tanji 1986; Gentilucci et al. 1988; Rizzolatti et al. 1988), distance from M1 DFL (Gentilucci et al. 1988), stimulation intensity to evoke movement (Hepp-Reymond et al. 1994), latencies for ICMS-evoked EMG activity (Boudrias and Cheney 2006) and pattern of cortical connections (Matelli et al. 1986; Barbas and Pandya 1987; Ghosh and Gattera 1995). It is thus tempting to

suggest that the squirrel monkey PMv DFL is the homolog of the macaque F5.

In sharp contrast to these similarities, the DFL of FR was found to be located much further rostral and lateral from the M1 DFL; required significantly higher current intensity to evoke movement; displayed evoked movements with much longer latencies; and had a different pattern of cortical connections. In particular, FR has sparse connections with M1 and numerous connections with prefrontal cortex and the AO. Taken together, these data lend support to the hypothesis that the squirrel monkey FR DFL is part of a separate cortical field, and is distinct from PMv areas that have been described previously.

The electrical stimulation properties and cortical connection patterns we found in FR are very similar to what has been described for pre-PMd and pre-SMA. Based on our data, one could conclude that FR is the "pre-PMv" of squirrel monkeys and that, as for pre-SMA and pre-PMd (Picard and Strick 2001), it should be considered a motor-related field providing an interface between prefrontal cortex and cortical motor areas, rather than a premotor area.

If FR is an additional motor-related field, it might be common to all primates. Specialized frontal fields appear to be unique in primate species, and well-conserved once established (Nudo and Frost 2006). Thus, it would be surprising to find this additional cortical subdivision of the lateral frontal cortex in squirrel monkeys and not in other primate species. Unfortunately it is very difficult to draw any conclusions from previous studies in other species as none of them were specifically designed to investigate the existence of an additional motor-related field rostral to PMv. However, in a few instances, studies in macaque monkeys have reported results that might suggest the existence of the macaque equivalent of FR. For example, as identified by ICMS techniques, a small isolated cluster of forelimb movement sites was reported far rostral and lateral on the caudo-ventral bank of the arcuate sulcus of a macaque monkey (case M57; Godschalk et al. 1995). In another ICMS study, in the cytoarchitectonically defined area 44, a site with orofacial and hand movement responses was found (Petrides et al. 2005). Finally, a functional imaging study in macaques has suggested the role of an architectonically defined field, the anterior sector of posterior bank or area F5a, in the coding of grasping (Nelissen et al. 2005).

In anatomical studies with other species, in some cases, it is clear that the PMv DFL has connections with the cortical areas rostral and lateral to it, where we found FR in the squirrel monkeys (Matelli et al. 1986; Kurata 1991; Fang et al. 2005). However, in all of these studies, the physiological documentation was restricted to PMv, making it difficult to argue against, or in favor of, the attribution of these connections to FR. In addition, as we previously stated (Dancause, Barbay, Frost, Plautz, Stowe, et al. 2006), several factors may account for the lack of reports in the literature of PMv connections with FR. The small size of our injections, the use of BDA (which is known to produce confined injection cores), the restriction of the injection to the distal forelimb area and the use of tangential sectioning may have allowed better visualization of FR.

In summary, the physiological and anatomical properties of FR suggest that it is a separate, motor-related field in squirrel monkeys. A comparable cortical area is expected to be present at least in other New World primates, and perhaps in other primate species. Based on its pattern of cortical connections, this area is likely to have a unique role in the integration of prefrontal and anterior opercular inputs for the elaboration of motor outputs.

Funding

Canadian Institutes of Health Research fellowship to N.D.; National Institutes of Health grant (NS30853) to R.N.; National Institute of Child Health and Human Development Center grant (HD02528); and Landon Center on Aging.

Notes

Conflict of Interest: None declared.

Address correspondence to Numa Dancause, P.T., Ph.D., Department of Neurology, University of Rochester Medical Center, 601 Elmwood Ave, Box 673, Rochester, NY 14642, USA. Email: Numa_Dancause @urmc.rochester.edu.

References

Barbas H, Pandya DN. 1987. Architecture and frontal cortical connections of the premotor cortex (area 6) in the rhesus monkey. J Comp Neurol. 256:211–228.

Bates JF, Goldman-Rakic PS. 1993. Prefrontal connections of medial motor areas in the rhesus monkey. J Comp Neurol. 336:211–228.

Boudrias M-H, Cheney PD. 2006. Contrasting motor output capabilities of the forelimb representation in SMA, PMd, PMv, and M1 in rhesus macaques. In: 2006 neuroscience meeting planner. Atlanta (GA): Society for Neuroscience.

Dancause N, Barbay S, Frost SB, Mahnken JD, Nudo RJ. 2007. Interhemispheric connections of the ventral premotor cortex in a new world primate. J Comp Neurol. 505:701–715.

Dancause N, Barbay S, Frost SB, Plautz EJ, Chen D, Zoubina EV, Stowe AM, Nudo RJ. 2005. Extensive cortical rewiring after brain injury. J Neurosci. 25:10167–10179.

Dancause N, Barbay S, Frost SB, Plautz EJ, Popescu M, Dixon PM, Stowe AM, Friel KM, Nudo RJ. 2006. Topographically divergent and convergent connectivity between premotor and primary motor cortex. Cereb Cortex. 16:1057–1068.

Dancause N, Barbay S, Frost SB, Plautz EJ, Stowe AM, Friel KM, Nudo RJ. 2006. Ipsilateral connections of the ventral premotor cortex in a new world primate. J Comp Neurol. 495:374–390.

Dancause N, Barbay S, Frost SB, Zoubina EV, Plautz EJ, Mahnken JD, Nudo RJ. 2006. Effects of small ischemic lesions in the primary motor cortex on neurophysiological organization in ventral premotor cortex. J Neurophysiol. 96:3506–3511.

Donoghue JP, Leibovic S, Sanes JN. 1992. Organization of the forelimb area in squirrel monkey motor cortex: representation of digit, wrist, and elbow muscles. Exp Brain Res. 89:1–19.

Dum RP, Strick PL. 1991. The origin of corticospinal projections from the premotor areas in the frontal lobe. J Neurosci. 11:667–689.

Dum RP, Strick PL. 2002. Motor areas in the frontal lobe of the primate. Physiol Behav. 77:677–682.

Dum RP, Strick PL. 2005. Frontal lobe inputs to the digit representations of the motor areas on the lateral surface of the hemisphere. J Neurosci. 25:1375–1386.

Fang PC, Stepniewska I, Kaas JH. 2005. Ipsilateral cortical connections of motor, premotor, frontal eye, and posterior parietal fields in a prosimian primate, Otolemur garnetti. J Comp Neurol. 490:305–333.

Frost SB, Barbay S, Friel KM, Plautz EJ, Nudo RJ. 2003. Reorganization of remote cortical regions after ischemic brain injury: a potential substrate for stroke recovery. J Neurophysiol. 89:3205–3214.

Fulton J. 1935. A note on the definition of the "motor" and "premotor" areas. Brain. 58:311–316.

Gallyas F. 1979. Silver staining of myelin by means of physical development. Neurol Res. 1:203–209.

Gentilucci M, Fogassi L, Luppino G, Matelli M, Camarda R, Rizzolatti G. 1988. Functional organization of inferior area 6 in the macaque monkey 1: Somatotopy and the control of proximal movements. Exp Brain Res. 71:475–490.

Ghosh S, Gattera R. 1995. A comparison of the ipsilateral cortical projections to the dorsal and ventral subdivisions of the macaque premotor cortex. Somatosens Mot Res. 12:359–378.
Godschalk M, Mitz AR, van Duin B, van der Burg H. 1995. Somatotopy of monkey premotor cortex examined with microstimulation. Neurosci Res. 23:269–279.
Gould HJ, 3rd, Cusick CG, Pons TP, Kaas JH. 1986. The relationship of corpus callosum connections to electrical stimulation maps of motor, supplementary motor, and the frontal eye fields in owl monkeys. J Comp Neurol. 247:297–325.
Gould HJ, 3rd, Kaas JH. 1981. The distribution of commissural terminations in somatosensory areas I and II of the grey squirrel. J Comp Neurol. 196:489–504.
He SQ, Dum RP, Strick PL. 1993. Topographic organization of corticospinal projections from the frontal lobe: motor areas on the lateral surface of the hemisphere. J Neurosci. 13:952–980.
Hepp-Reymond MC, Husler EJ, Maier MA, Ql HX. 1994. Force-related neuronal activity in two regions of the primate ventral premotor cortex. Can J Physiol Pharmacol. 72:571–579.
Jain N, Qi HX, Catania KC, Kaas JH. 2001. Anatomic correlates of the face and oral cavity representations in the somatosensory cortical area 3b of monkeys. J Comp Neurol. 429:455–468.
Krubitzer LA, Kaas JH. 1990. The organization and connections of somatosensory cortex in marmosets. J Neurosci. 10:952–974.
Kurata K. 1991. Corticocortical inputs to the dorsal and ventral aspects of the premotor cortex of macaque monkeys. Neurosci Res. 12:263–280.
Kurata K, Tanji J. 1986. Premotor cortex neurons in macaques: activity before distal and proximal forelimb movements. J Neurosci. 6:403–411.
Lu MT, Preston JB, Strick PL. 1994. Interconnections between the prefrontal cortex and the premotor areas in the frontal lobe. J Comp Neurol. 341:375–392.
Luppino G, Matelli M, Camarda RM, Gallese V, Rizzolatti G. 1991. Multiple representations of body movements in mesial area 6 and the adjacent cingulated cortex: an intracortical microstimulation study in the macaque monkey. J Comp Neurol. 311:463–482.
Luppino G, Matelli M, Camarda R, Rizzolatti G. 1993. Corticocortical connections of area F3 (SMA-proper) and area F6 (pre-SMA) in the macaque monkey. J Comp Neurol. 338:114–140.
Mao CC, Coull BM, Golper LA, Rau MT. 1989. Anterior operculum syndrome. Neurology. 39:1169–1172.
Matelli M, Camarda R, Glickstein M, Rizzolatti G. 1986. Afferent and efferent projections of the inferior area 6 in the macaque monkey. J Comp Neurol. 251:281–298.
Matelli M, Luppino G, Rizzolatti G. 1985. Patterns of cytochrome oxidase activity in the frontal agranular cortex of the macaque monkey. Behav Brain Res. 18:125–136.
Matelli M, Luppino G, Rizzolatti G. 1991. Architecture of superior and mesial area 6 and the adjacent cingulate cortex in the macaque monkey. J Comp Neurol. 311:445–462.
Morecraft RJ, Van Hoesen GW. 1992. Cingulate input to the primary and supplementary motor cortices in the rhesus monkey: evidence for somatotopy in areas 24c and 23c. J Comp Neurol. 322:471–489.
Murata A, Fadiga L, Fogassi L, Gallese V, Raos V, Rizzolatti G. 1997. Object representation in the ventral premotor cortex (area F5) of the monkey. J Neurophysiol. 78:2226–2230.
Nelissen K, Luppino G, Vanduffel W, Rizzolatti G, Orban GA. 2005. Observing others: multiple action representation in the frontal lobe. Science. 310:332–336.
Nudo RJ, Frost SB. 2006. The evolution of motor cortex and motor systems. In: Krubitzer LA, Kaas JH, editors. Evolution of nervous systems in mammals. Oxford (UK): Elsevier.
Nudo RJ, Jenkins WM, Merzenich MM, Prejean T, Grenda R. 1992. Neurophysiological correlates of hand preference in primary motor cortex of adult squirrel monkeys. J Neurosci. 12:2918–2947.
Nudo RJ, Larson D, Plautz EJ, Friel KM, Barbay S, Frost SB. 2003. A squirrel monkey model of poststroke motor recovery. Ilar J. 44:161–174.
Nudo RJ, Masterton RB. 1990. Descending pathways to the spinal cord, 3: Sites of origin of the corticospinal tract. J Comp Neurol. 296:559–583.
Owen AM. 1997. The functional organization of working memory processes within human lateral frontal cortex: the contribution of functional neuroimaging. Eur J Neurosci. 9:1329–1339.
Petrides M. 1995. Impairments on nonspatial self-ordered and externally ordered working memory tasks after lesions of the mid-dorsal part of the lateral frontal cortex in the monkey. J Neurosci. 15:359–375.
Petrides M, Cadoret G, Mackey S. 2005. Orofacial somatomotor responses in the macaque monkey homologue of Broca's area. Nature. 435:1235–1238.
Picard N, Strick PL. 1996. Motor areas of the medial wall: a review of their location and functional activation. Cereb Cortex. 6:342–353.
Picard N, Strick PL. 2001. Imaging the premotor areas. Curr Opin Neurobiol. 11:663–672.
Preuss TM, Goldman-Rakic PS. 1989. Connections of the ventral granular frontal cortex of macaques with perisylvian premotor and somatosensory areas: anatomical evidence for somatic representation in primate frontal association cortex. J Comp Neurol. 282:293–316.
Preuss TM, Stepniewska I, Kaas JH. 1996. Movement representation in the dorsal and ventral premotor areas of owl monkeys: a microstimulation study. J Comp Neurol. 371:649–676.
Reiner A, Veenman CL, Medina L, Jiao Y, Del Mar N, Honig MG. 2000. Pathway tracing using biotinylated dextran amines. J Neurosci Methods. 103:23–37.
Rizzolatti G, Camarda R, Fogassi L, Gentilucci M, Luppino G, Matelli M. 1988. Functional organization of inferior area 6 in the macaque monkey. 2. Area F5 and the control of distal movements. Exp Brain Res. 71:491–507.
Rizzolatti G, Fogassi L, Gallese V. 2001. Neurophysiological mechanisms underlying the understanding and imitation of action. Nat Rev Neurosci. 2:661–670.
Rolls ET. 1989. Information processing in the taste system of primates. J Exp Biol. 146:141–164.
Sakai ST, Stepniewska I, Qi HX, Kaas JH. 2000. Pallidal and cerebellar afferents to presupplementary motor area thalamocortical neurons in the owl monkey: a multiple labeling study. J Comp Neurol. 417:164–180.
Shimazu H, Maier MA, Cerri G, Kirkwood PA, Lemon RN. 2004. Macaque ventral premotor cortex exerts powerful facilitation of motor cortex outputs to upper limb motoneurons. J Neurosci. 24:1200–1211.
Stoney SD, Jr, Thompson WD, Asanuma H. 1968. Excitation of pyramidal tract cells by intracortical microstimulation: effective extent of stimulating current. J Neurophysiol. 31:659–669.
Strick PL, Preston JB. 1982. Two representations of the hand in area 4 of a primate. 1. Motor output organization. J Neurophysiol. 48:139–149.
Tanné-Gariépy J, Rouiller EM, Boussaoud D. 2002. Parietal inputs to dorsal versus ventral premotor areas in the macaque monkey: evidence for largely segregated visuomotor pathways. Exp Brain Res. 145:91–103.
Vogt C, Vogt O. 1919. Allgemeinere Ergebnisse unserer Hirnforschung. J Psychol Neurol. 25(suppl 1):273–462.
Von Bonin G, Bailey P. 1947. The neocortex of Macaca mulatta. Urbana (IL): University of Illinois Press.
Wise SP. 2006. The ventral premotor cortex, corticospinal region C, and the origin of primates. Cortex. 42:521–524.